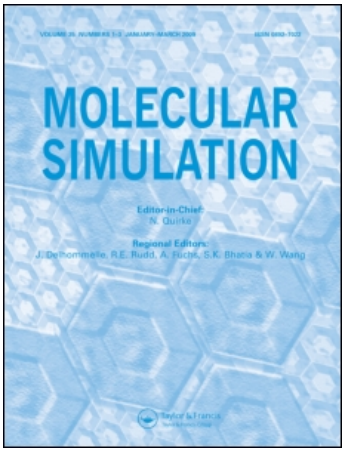

Molecular Simulation
Publication details, including instructions for authors and subscription information:
http://www.informaworld.com/smpp/title~content=t713644482

Computer simulation of calcite growth inhibition: A study of monophosphonate interaction with calcite

Sonia A. Ojo[a]; B. Slater[a]; C. R. A. Catlow[a]
[a] Davy Faraday Research Laboratory, The Royal Institution of Great Britain, London, UK

Online publication date: 26 October 2010

To cite this Article Ojo, Sonia A. , Slater, B. and Catlow, C. R. A.(2002) 'Computer simulation of calcite growth inhibition: A study of monophosphonate interaction with calcite', Molecular Simulation, 28: 6, 591 — 606
To link to this Article: DOI: 10.1080/08927020290030152
URL: http://dx.doi.org/10.1080/08927020290030152

Molecular Simulation, 2002 VOL. 28 (6-7), pp. 591–606

COMPUTER SIMULATION OF CALCITE GROWTH INHIBITION: A STUDY OF MONOPHOSPHONATE INTERACTION WITH CALCITE

SONIA A. OJO, B. SLATER and C.R.A. CATLOW

Davy Faraday Research Laboratory, The Royal Institution of Great Britain, 21 Albemarle Street, London, W1S 4BS, UK

(Received May 2001; Accepted August 2001)

We have performed atomistic surface simulations of the interaction of monophosphonate growth inhibitor ions with the planar and obtuse stepped $\{10\bar{1}4\}$ surfaces of calcium carbonate. We show that phosphonate inhibitor ions have a smaller adsorption energy on the planar $\{10\bar{1}4\}$ surface compared to the obtuse stepped $\{10\bar{1}4\}$ surface in accordance with experiment; and that the binding energy of the inhibitor with the surface is dominated by electrostatic forces. We find that replacement processes which simulate the irreversible incorporation of monophosphonate ions at terrace and step sites are energetically more favourable than those calculated for the diphosphonate ion. The inhibition mechanism proposed to operate for the deprotonated monophosphonate/calcite system is *via* the binding or incorporation of monophosphonate ions to the calcite obtuse step sites and kink sites thus slowing step flow and thereby destroying and/or delaying the formation of potential kink sites and step assembly.

Keywords: Calcite; Inhibition; Monophosphonate ions

INTRODUCTION

A plethora of studies has been reported on the inhibition of calcite growth by organic as well as inorganic ions. The motivation for the work arises to a large extent from operational problems in the oil and water industries [1] in both of

*.

ISSN 0892-7022 © 2002 Taylor & Francis Ltd
DOI: 10.1080/08927020290030152

which calcite scale build-up is a major operational hazard. Some of the most widely used inhibitors are organic phosphonate ions and it is considered that diphosphonates and polyphosphonates are more efficient crystal growth poisons than monophosphonates. It is generally accepted that it is the phosphonate head group that interferes with the nucleation and growth process, preventing step flow and propagation, thereby inhibiting growth and augmenting the crystal morphology.

A previous study by Nygren *et al*. [2] demonstrated how atomistic computer simulation techniques could be used to model the interaction of diphosphonate inhibitors with defects in terrace and step sites on the $\{10\bar{1}4\}$ surface of calcite. They showed that it was unlikely for a diphosphonate ion to become incorporated into the calcite framework by the simultaneous blocking of step and terrace sites. Instead, they proposed that a diphosphonate ion was more likely to become reversibly bound to the calcite framework, thereby inhibiting crystal growth by preventing successive adsorption of $CaCO_3$ units.

The present study builds on this previous work by simulating a variety of monophosphonate inhibitor ions at terrace and step defect sites, (illustrated in Fig. 1), to develop models for the inhibition mechanism and its dependence on the structural properties of the inhibitor molecules.

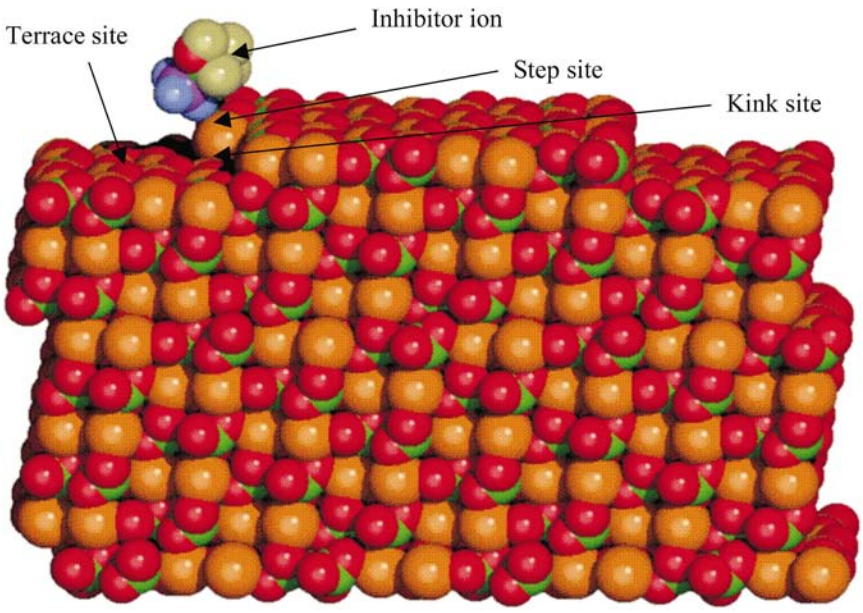

FIG. 1 Schematic of the terrace, step and kink sites at a calcite $\{10\bar{1}4\}$ surface with inhibitor ion approaching kink site. N.B. Ca: orange, carbonate O: red, ion O: blue, H: taupe, P: mauve, C: green.

EXPERIMENTAL AND COMPUTATIONAL BACKGROUND

The effects of phosphonate poisons on crystal growth and morphology have been studied by numerous workers including Brooks *et al*. [3]. Growth inhibition processes have been identified by Hatch and Rice [4] and Reitmeier and Buehrer [5] as surface controlled events which require a very small concentration of poison to inhibit crystal formation; these observations were supported much later by Nancollas *et al*. [6] and Weigen *et al*. [7]. This surface controlled crystal growth mechanism was later shown to have a rate determining step governed by the rate of kink formation [8].

Techniques such as Atomic Force Microscopy(AFM) have been used to understand the molecular basis of the models for the inhibition mechanism [9]. Gratz *et al*. and Hillner *et al*. [10–12] observed the crystal growth inhibition process, by performing real-time, *in situ* AFM imaging; they found accumulation of HEDP at the step-edge sites of the calcite crystal rather than terrace sites.

Although the processes involved in crystal growth inhibition are acknowledged as complex, there is a general consensus that the three main factors that influence the degree of interaction between organic phosphate containing compounds with various calcite crystal planes are *charge distribution*, *steriochemistry* and *geometry* as reported by Davey [13], Mann *et al*. [14] Austin *et al*. [15] and Teng *et al*. [16]. It is also clear that the inhibition is strongly determined by external factors such as pH, temperature and supersaturation.

Additionally, inhibitor efficacy can be substantially enhanced by the functional groups within the structural framework of the poison [17–21], as will be underlined by the calculations reported in this study. Indeed, the phosphonates in this work were selected to investigate the extent to which electrostatic interactions between phosphonates and calcite surfaces were enhanced or decreased by functional groups, which may donate or withdraw electron density from the phosphonate oxygen.

Over the last decade, atomistic simulation techniques have made a major contribution to the elucidation of mineral crystal growth phenomena [22]. Simulations of cation/anion impurities, hydration effects on mineral growth and morphology, which agree well with experiment have been reported [23–26]. This work provides a firm foundation for this study.

METHOD

Phosphonates Used in This Study

The five phosphonates modelled during this work are listed in Table I. HEMP, DMP and PEMP are the mono-substituted analogues of the diphosphonates

TABLE I Five phosphonate ions modelled in this work (N.B. The charge neutral analogue of each phosphonate was used in the binding calculations)

HEDP:	$[(PO_3)_2CH(CH_3)(OH)]^{4-}$
HEMP:	$[(PO_3)CH(CH_3)(OH)]^{2-}$
DMP:	$[(PO_3)CH(OH)_2]^{2-}$
PEMP:	$[(PO_3)CH(CH_3)_2]^{2-}$
PMP:	$[(PO_3)Ph]^{2-}$

previously modelled [2]. HEDP and PMP were chosen to compare with existing experimental data. HEMP exhibits a methyl and a hydroxyl group; PEMP contains two methyl groups, whilst DMP has two hydroxyl groups; HEDP is the diphosphonate analogue of HEMP ion whist PMP contains a phenyl group attached to the phosphonate motif.

Modelling of these five inhibitors with the calcite surface will allow us to investigate the impact of both steric and electrostatic factors on inhibition mechanisms.

Description of Charges

A key requirement for modelling phosphonate ions is to achieve a suitable representation of the charge distribution. In the present work, the method of Gasteiger *et al*. [27] available within *Cerius* ^{2} [28] package was employed, as this method gave equal charge distribution on all the oxygen atoms of the phosphonate group. Comparison with charge distributions from semi-empirical methods (AM1, PM3, and MNDO) gave comparable charge distributions (reported elsewhere) [29] and supported the charge assignment used in our simulations of the phosphonate ions. Note that for the binding calculations, we have fully deprotonated the ion and redistributed charge over the absorbate in a consistent manner (using the Gasteiger method), thus rendering the "ion" charge neutral. In the replacement calculations, the ions retain their original net charge.

Simulation Techniques

Modelling of surfaces was achieved using MARVINS Program [30] that simulates the surface using a two-dimensional cell consisting of a lower, fixed region of atoms representing the bulk and an upper region containing several layers of atoms that are allowed to relax. The long-range electrostatic interactions are described in terms of a 2-D Ewald summation. The extended MARVINS code used within this work includes a molecular dynamics routine.

Full details of the simulation parameters are reported elsewhere [29]. Dynamical calculations of solvated inhibitor ions were performed with the *Discover*® program [28] employing the molecular mechanics CVFF forcefield. We used the Born-model potential developed by Pavese *et al*. [31] to represent calcite in which Ca^{2+} and CO_3^{2-} ions are assigned formal charges.

Before docking each phosphonate on the calcite surface, we performed an energy minimization on the inhibitor molecule. The phosphonates were then randomly "docked" onto the planar calcite $\{10\bar{1}4\}$ surface. The entire system was then energy minimized and subjected to 20 ps of constant temperature molecular dynamics at 298 K. The simulations yielded a catalogue of conformations; the three of lowest energy were extracted for further energy minimizations, in order to generate the most favourable energy conformation. This procedure was repeated for the obtuse stepped $\{10\bar{1}4\}$ surface/phosphonate systems and in the calculation of replacement energies.

Note that in our docking and replacement calculations the surface is performed *in vacuo*: there is no explicit representation of the water solvent. Whilst recent work [23] indicates that water has a strong effect on step and kink formation energies, our calculations have neglected this factor as a first approximation. Since the formation of surface complexes is likely to be dictated largely by the electrostatic forces acting between the surface and the adsorbate, we consider that comparison of relative absorption/replacement energies in the absence of solvent should give qualitatively correct trends.

Reaction Schemes

Following previous work [2], the following reaction schemes may be proposed for the replacement by a monophosphonate ion of surface CO_3^{2-} species:

$$CO_3^{2-}\,(\text{surface}) + \text{monoPO}_3^{2-}\,(\text{solution}) \rightarrow CO_3^{2-}\,(\text{solution}) + \text{monoPO}_3^{2-}\,(\text{surface}),$$

for which the corresponding replacement energy is given by:

$$E_{\text{replacement}} = E_{\text{solution}}(CO_3)^{2-} + E_{\text{surface}}\,(\text{monoPO}_3)^{2-} - E_{\text{solution}}\,(\text{monoPO}_3)^{2-} - E_{\text{surface}}\,(CO_3)^{2-}$$

which requires an estimate of the solvation energies. These latter calculations were performed in an identical to fashion to that described by Nygren *et al*. and the solvation energies are shown in Table II.

TABLE II Calculated solvation energies of anionic phosphonate ions. Simulations were performed using *DISCOVER* ® and included energy minimization and 15 ps of molecular dynamics performed at 298 K

Phosphonate ion	*Solvation energy*/kJ mol^{-1}
$[HEDP]^{4-}$	3079.8
$[HEMP]^{2-}$	1367.2
$[DMP]^{2-}$	1414.4
$[PEMP]^{2-}$	1275.5
$[PMP]^{2-}$	797.9
$[CO_3]^{2-}$	1109.6

RESULTS

We firstly verified the result of Nygren *et al*. regarding replacement of HEDP at the calcite terrace (described fully elsewhere [29]). The calculated equilibrium distance between the phosphonate groups within the HEDP ion of 4.1 Å is close to the shortest carbonate–carbonate calcite distances of 4.05 Å. Substitution of two carbonates ions for HEDP at larger separations of 4.80 and 6.29 Å gave very unfavourable replacement energies of 336.7 and 1154.0 kJ/mol^{-1}. However, even the most favourable calculated replacement energy of 43.4 kJ/mol^{-1} (for carbonate ions separated by 4.05 Å), suggests that permanent occlusion into calcite using *two* fully deprotonated phosphonate moieties would be thermodynamically forbidden. The experimental literature is inconclusive on this crucial point, since external factors such as pH play a major role. However, we speculate that one singly protonated phosphonate group may be required to facilitate optimum binding of a diphosphophosphonate to calcite whilst one fully deprotonated phosphonate group becomes incorporated *via* CO_3 replacement.

Monophosphonate Absorption At the Ideal and Obtuse Stepped Calcite {10$\bar{1}$4} Surfaces

The binding energy of a neutral phosphonate species with respect to the planar {10$\bar{1}$4} calcite surface which contained no defects, was calculated for all five phosphonates; the results are reported in Table III.

All calculated binding energies were favourable and their magnitude suggests that the inhibitors will physisorb rather than chemisorb to the planar surface. The negative binding energy for HEDP reinforces the concept that *binding* rather than *incorporation* is the dominant mode of interaction to the planar surface.

Analysis of the simulations showed that the phosphonate ions were predominantly bound *via* electrostatic attraction between the oxygen atoms of

TABLE III Calculated binding energies for the phosphonate ions at the planar $\{10\bar{1}4\}$ surface after 20 ps NAT dynamics performed at 298 K

Phosphonate	*Binding Energy*/kJ mol^{-1}
HEDP	85.9
HEMP	54.0
DMP	47.3
PEMP	41.5
PMP	18.4

the phosphonate group and the surface. Trends within the calculated binding energies are also consistent with the idea that surface binding is dominated by the phosphonate group; the binding energy of the diphosphonate is approximately twice that of the monophosphonates (with the exception of PMP). Fig. 2 shows a typical configuration, at the end of an MD simulation; the oxygen atoms of the phosphonate group bind with the calcium atoms, whilst in the case of DMP and

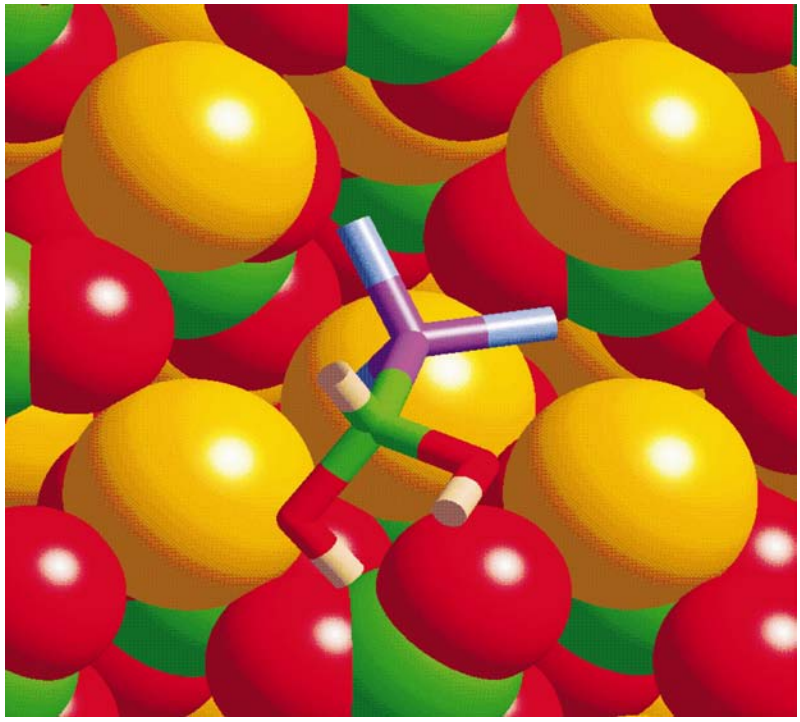

FIG. 2 A DMP ion at the planar calcite surface after simulation. N.B. for calcite surface Ca: yellow, carbonate O: red, C: green, phosphonate O: light blue, hydroxyl oxygen: red, P: mauve, H: taupe.

TABLE IV Calculated binding energies for the phosphonate ions at the stepped calcite plane after 20 ps NAT dynamics performed at 298 K

Phosphonate	*Binding Energy*/kJ mol^{-1}
HEDP	−276.0
HEMP	−166.9
DMP	−182.4
PEMP	−140.9
PMP	−118.7

HEMP, the hydroxyl oxygen atom orients to maximize electrostatic binding with the Ca^{2+} sites.

Next we calculated binding energies for the phosphonates at the stepped $\{10\bar{1}4\}$ calcite surface; the results are given in Table IV.

The phosphonates are more strongly bound to the stepped surface compared to the planar surface as has been predicted and observed experimentally [9]. The phosphonate group binds electrostatically with the step edge and additional stabilisation may be facilitated by the side groups binding to the step. Indeed, the calculated binding energies were approximately three-times those previously calculated on the planar $\{10\bar{1}4\}$ surface. We note that PMP has the lowest calculated binding energy since the phenyl ring is repelled by the step edge, whilst DMP and HEMP possess polar oxygen atoms within hydroxyl groups which increase the binding to calcite by approximately 20–40 kJ/mol^{-1} (relative to PEMP).

Incorporation of Monophosphonate Ions into Terrace, Steps and Step Edge Defect Sites

We now investigate the interaction of the monophosphonates with defect sites created by the removal of carbonate ions from both the terrace and step as well as the "edge" (lower step) sites of the stepped surface, as illustrated in Fig. 3.

In order to compare possible mechanisms of monophosphonate crystal growth inhibition, we have simulated two processes. The models investigated were substitution (or replacement) of the inhibitor into a terrace, step or edge defect site and binding of a $CaCO_3$ unit next to pre-docked monophosphonate ions at a kink. The latter model is necessary to establish which inhibitor would be more damaging to the actual step assembly and flow rate.

The calculated replacement energies reported in Table V are mostly negative and therefore represent favourable occlusion of the impurity into the calcite surface. Overall the impurities at the stepped site yielded the most favourable replacement energies for ions other than PMP. In accordance with AFM studies

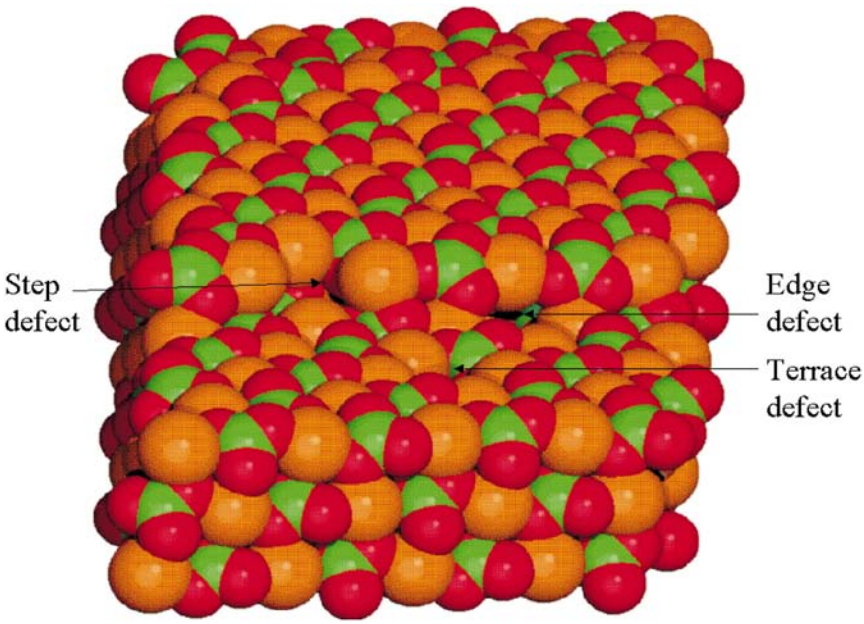

FIG. 3 Schematic showing sites of the three surface defects.

[9], it was observed that the primary location of the diphosphonate ion, HEDP, was in the vicinity of the step. The only favourable replacement energy calculated for the PMP ion was at the terrace site (Fig. 4), due principally to the steric bulk and electrostatic properties of the phenyl group. This is shown by the phenyl group being slightly repelled by the calcite step.

We found that monophosphonates are preferentially incorporated at step sites. Overall, the DMP ion was observed to form the closest contacts with the calcite surface, due to the polar nature of the hydroxyl groups, compared to the bulky methyl and phenyl groups present in the other ions.

From the calculated favourable replacement energies we suggest that substitution of a carbonate ion by a monophosphonate ion into the calcite

TABLE V Calculated replacement energies/ kJmol^{-1} at the obtuse step $\{10\bar{1}4\}$ stepped calcite plane (EDGE = lower step site, see Fig. 3)

Defect	HEDP	HEMP	DMP	PEMP	PMP
STEP	695.65	51.14	− 386.99	− 235.42	− 362.78
TERRACE	695.65	− 89.92	− 308.75	− 176.56	− 111.92
EDGE	N/A	261.14	− 215.16	134.14	− 75.16

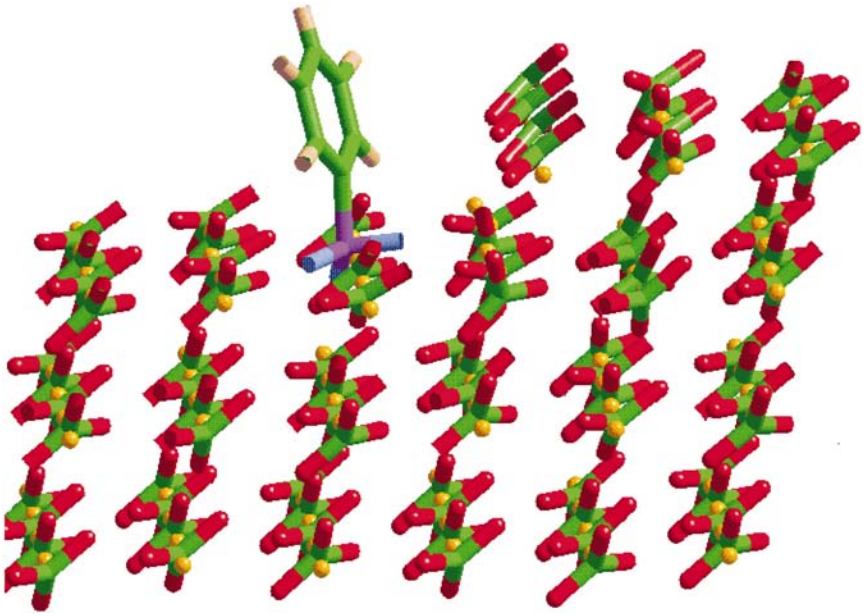

FIG. 4 PMP, at a step defect, after 5 ps of constant temperature dynamics performed at 298 K using MARVIN.

framework at either step or terrace sites are feasible mechanisms and we suggest that binding at both sites operates to prevent crystal growth.

Binding of $CaCO_3$ Kink Sites to Obtuse Steps Containing Phosphonate Inhibitor Ions

Another proposed mechanism of crystal growth inhibition is *via* kink site annihilation [2,13] by a monophosphonate ion. Further details of the simulation conditions and methodology are reported elsewhere [29]. In essence, the calculation scheme mirrors the formation of a step. Initially, a single $CaCO_3$ unit was bound and relaxed to equilibrium at the step. An impurity is bound adjacent to the first unit, and a second $CaCO_3$ is bound next to that. The calculated binding energies of $CaCO_3$ units bound next to a variety of ions are reported in Table VI. We recall that binding an impurity ion to a step site has been found to be a favourable process with negative binding energies obtained for all ions, (Table IV). A comparison with the binding energies of $CaCO_3$, Table VI, at stepped sites show this process to be considerably more favourable.

From Table VI, it can be established that the process of binding successive $CaCO_3$ units to a step is more energetically feasible in a pure crystal and a

TABLE VI Calculated binding energies of $CaCO_3$ units bound to kink sites containing phosphonate ions at the stepped{$10\bar{1}4$} surface

Kink ion	Binding energy/ kJ mol^{-1}
$CaCO_3$, first	− 955.2
$CaCO_3$, second	− 1539.9
HEDP	− 22.2
HEMP	− 113.8
DMP	− 124.5
PEMP	− 104.2
PMP	− 226.7

substantially more exothermic process, when compared to a poisoned crystal in which $CaCO_3$ units have inhibitors as neighbours. We propose from these results that the formation of the kink site is frustrated by the presence of the monophosphonate ion. We note that if the method used to calculate binding energies in Table VI were explicitly to include solvation effects, the effect of binding a $CaCO_3$ next to a pre-bound inhibitor would probably be an endothermic process, suggesting that further growth at a poisoned step would become energetically unfeasible and therefore step assembly and flow would cease altogether.

DISCUSSION AND CONCLUSION

The mechanisms by which a phosphonate ion could hinder crystal growth can be grouped as follows: binding to a terrace, step or kink site and/or incorporation of the inhibitor into terrace, obtuse step or kink sites. In the following sections we compare the viability of these processes for mono and diphosphonates and their impact on crystal growth and morphology.

Inhibition Mechanisms for Mono and Diphosphonates: Binding Versus Replacement

Our results indicate that binding, which is dominated by electrostatic attraction between the phosphonate oxygen atoms and Ca^{2+} sites, is an energetically favourable process for both mono and diphosphonates, at terraces, steps and kink sites. Furthermore, binding becomes more favourable at sites with higher electrostatic potential, reflected by the increase in binding energies for terrace, step and kink sites respectively. If we examine the energies, we find that for both mono and diphosphonates, binding to terrace sites is favourable, and the energies

are consistent with physisorption; since the inhibitor would be bound transiently, it is unlikely that this mode of interaction would lead to retardation of crystal growth *per se*.

At step sites, the binding energies are indicative of chemisorption. Therefore competition between the poison and $CaCO_3$ for nucleation sites will occur, and we anticipate that mono and diphosphonates will slow crystal growth. The magnitude and composition of the binding energy for mono and diphosphonates shows that diphosphonates bind approximately twice as strongly as monophosphonates simply because they possess two rather than one phosphonate group.

We find that monophosphonate ions can irreversibly incorporate into the calcite surface at terrace or obtuse stepped sites, whilst for HEDP, replacement is an *endothermic* process. The pH will clearly affect the degree of protonation and hence the energetics of incorporation; we plan to investigate this aspect more thoroughly using techniques which permit charged simulation cells.

We found that the binding of a $CaCO_3$ unit to a pre-docked inhibitor ion (attached to a kink) is much less than that of a $CaCO_3$ unit next to a kink. The presence of the inhibitor at the kink site clearly acts as a barrier for the attachment of further $CaCO_3$. Our results clearly identify that monophosphonates would be inferior to HEDP, which can be attributed in part to steric factors and screening properties of HEDP compared to the monphosphonates. We would expect the kink–kink annihilation velocity to decrease, due to the phosphonate poisons sterically hindering access and growth at the defect sites, leading to decreased step assembly and flow. In fact, according to Davey [13], desorption of an inhibitor bound to the kink site would require surmounting such a huge activation energy that the kink site would be rendered totally inactive for further growth. This process would give rise to observable jagged steps, which has indeed been found experimentally [9,32]. Therefore, we suggest that at high concentrations, fully deprotonated monophosphonates impede crystal growth and alter crystal morphology by: (i) binding to step sites, (ii) poisoning kink sites thus rendering them inactive and (iii) becoming occluded to the step *via* a replacement process.

HEDP is unlikely to replace two carbonate defects in concert due to entropic effects, and energetic considerations (shown in Table V). However, we infer that incorporation of a single phosphonate and binding of the remaining phosphonate group to calcium sites would be favourable, since both binding and replacement of a single phosphonate group have been shown to be energetically favourable processes (Tables III–V).

The diphosphonate ion, HEDP, is more effective at preventing step assembly at kink nucleation sites (Table VI) compared to the monophosphonate ions and exhibits superior potency due its ability to bind strongly to the step (Table IV) and to reduce binding of further growth units.

Phosphonate Binding As a function of Structure

All phosphonate ions, bind to the terrace/step/kink or incorporate *via* the tripod of oxygen atoms of the phosphonate motif (Figs. 2 and 4). The dihydroxy-substituted ion, DMP, binds additionally using the oxygen atom of an hydroxyl, to co-ordinate to a calcium ion at a step site, further stabilising the surface/poison complex, which is reflected in the relatively large binding energy in Table V. The PMP inhibitor has an inflexible phenyl ring, the steric bulk of which prevents favourable replacement at step sites. Additionally, the phenyl ring withdraws electron density away from the phosphophosphonate group oxygen atoms thus reducing the strength of electrostatic attraction between the poison and the calcite surface; hence the fully deprotonated PMP is the most weakly bound monophosphonate (Tables III and IV) and consequently would be expected to be a less potent inhibitor

Correlation With Experiment

Experimental studies [14,33] have shown that the calcite morphology is altered by PMP. We suggest that the distortions reported, exemplified by curved steps for instance, may arise from PMP binding at kink sites and becoming incorporated in terraces. In both cases, $CaCO_3$ units would bind weakly next to the impurity, giving rise to distorted steps. Incorporation into terraces would result in step pinning, where the advancing step is "caught" by the inhibitor obstruction. Permanent binding to kink sites would give rise to large gaps between kink sites due to steric factors and retarded step assembly. Clearly, any or all of these phenomena would lead to the observed distortions at steps. More generally, we note that the binding and incorporation mechanisms for PMP are the least favourable of all the phosphonates studied, and in agreement with observation, this inhibitor is relatively ineffectual. Given that the singly protonated phosphonate moiety has been found to be more effective our results do not conflict with Mann *et al*. [33] who suggested that this poison stabilises the $\{01\bar{1}2\}$ plane rather than destabilising the $\{10\bar{1}4\}$ plane.

In the case of non-aromatic monophosphonates, the exothermic replacement and large binding energies calculated showed the step site to be a favourable location for this process, a result which has been corroborated for the diphosphonate, HEDP using AFM [11,12]. For HEDP, our calculations suggest that replacement is not viable at the obtuse step, but bi-dentate binding and uni-dentate replacement with uni-dentate binding is energetically favourable at step sites, in agreement with the previous AFM observations.

We note that phosphonate inhibition is at a maximum between pH 5 and 7 when singly protonated phosphonate groups are likely to be present in higher concentrations thus permitting hydrogen bonding to the calcite surface; hence in this pH range, HEDP and PMP have been shown to be more potent in smaller concentrations. Under acidic conditions, although the inhibitor ions may potentially bind to the calcium sites, the electron density on the phosphonate oxygen will be less than that in basic conditions. Therefore all the phosphonate inhibitors studied would be expected to be far less effective at retarding step flow/assembly and hence reducing crystal growth. We have already noted that these morphological effects are concentration, temperature and pH dependent and hence further work encompassing these effects would provide a more detailed description of inhibition phenomena.

SUMMARY

Simulations of irreversible incorporation and reversible binding of four monophosphonate ions and HEDP to terraces, obtuse steps and kinks on the $\{10\bar{1}4\}$ calcite surface have been used to rationalise experimental observations using mechanistic and electrostatic arguments. Step and kink sites are the primary areas of phosphonate inhibition activity resulting in a decrease and/or stoppage of step flow and assembly. We find that the diphosphonate, HEDP is a more powerful poison than the four monophosphonates modelled, as demonstrated by their respective calculated binding energies. The presence of heteroatoms, such as oxygen was shown to enhance electrostatic attraction to calcium atoms, resulting in increased binding to the calcite lattice. The aromatic ring in PMP was found to degrade poison efficacy due to reduced phosphonate oxygen basicity and steric factors. We find that it is more energetically feasible for a single phosphonate moiety to become incorporated into the calcite lattice rather than dual phosphonate substitution in the case of HEDP.

Acknowledgements

Financial support for this work by EPSRC is gratefully acknowledged. We thank Accelrys for the use of the *Cerius*^{2} and *Discover*® codes.

References

[1] Rankin, A.H. and Sutcliffe, P.J.C. (1999) "Morphology, chemistry and growth mechanisms of calcite concretions from an industrial water-softening process: implications for the origin of natural ooids in sediments", *Proceedings of the Geologists Association* **110**, 33.

[2] Nygren, M.A., Gay, D.H., Catlow, C.R.A., Wilson, M.P. and Rohl, A.L. (1998) "Incorporation of growth-inhibiting diphosponates into steps on the calcite cleavage plane", *J. Chem. Soc., Faraday Trans.* **94**, 3685.
[3] Brooks, R., Clark, L.M. and Thurston, E.F. (1950), *Philo. Trans. R. Soc. London, Ser. A* **243**, 145.
[4] Hatch, G.B. and Rice, O. (1939), *Ind. And Eng. Chem.* **31**, 54.
[5] Reitemeier, R.F. and Buehrer, T.F. (1940), *J. Phys. Chem.* **44**, 535.
[6] Nancollas, G.H., Kazmierczak, T.F. and Schuttringer, E. (1981) "A controlled composition study of calcium–carbonate crystal-growth—the influence of scale inhibitors", *Corrosion* **37**, 76.
[7] Weigen, M.P.C., Marchee, W.G.J. and van Rosmalen, G.M. (1983) "A quantification of the effectiveness of an inhibitor on the growth-process of a scalant", *Desalination* **47**, 81.
[8] Christoffersen, J. and Christoffersen, M.R. (1990) "Kinetics of spiral growth of calcite crystals and determination of the absolute rate-constant", *J. Crystal Growth* **203**, 100.
[9] Gratz, A.J., Hillner, P.E. and Hansma, P.K. (1993) "Step dynamics and spiral growth on calcite", *Geochimica et Cosmochimica Acta.* **57**, 491.
[10] Hillner, P.E., Gratz, A.J. and Manne, S. (1992) "Atomic-scale imaging of calcite growth and dissolution in real-time", *Geology* **20**, 359.
[11] Hillner, P.E., Manne, S., Hansma, P.K. and Gratz, A.J. (1993) "Atomic-force microscope—a new tool for imaging crystal-growth processes", *Faraday Discuss.* **95**, 191.
[12] Gratz, A.J. and Hillner, P.E. (1993) "Poisoning of calcite growth viewed in the atomic force microscope (AFM)", *J. Crystal Growth* **129**, 789.
[13] Davey, R.J. (1976), *J. Crystal Growth* **34**, 109.
[14] Mann, S., Archibald, D., Didymus, J.M., Douglas, T., Heywood, B.R., Meldrum, F.C. and Reeves, N.J. (1993) "Crystallization at inorganic–organic interfaces—biominerals and biomimetic synthesis", *Science* **261**, 6.
[15] Austin, A.E., Miller, J.F., Vaughan, D.A. and Kircher, J.F. (1975), *Desalination* **16**, 345.
[16] Teng, H.H., Dove, P.M., Orme, C.A. and DeYoreo, J.J. (1998) "Thermodynamics of calcite growth: Baseline for understanding biomineral formation", *Science* **282**, 5389.
[17] Rohl, A.L., Gay, D.H., Davey, R.J. and Catlow, C.R.A. (1996) "Interactions at the organic/inorganic interface: Molecular modeling of the interaction between diphosphonates and the surfaces of barite crystals", *J. Am. Chem. Soc.* **118**, 642.
[18] Black, S.N., Bromley, L.A., Cottier, D., Davey, R.J., Dobbs, B. and Rrout, J.E. (1991) "Interactions at the organic inorganic interface—binding motifs for phosphonates at the surface of barite crystals", *J. Chem. Soc. Faraday Trans.* **87**, 3409.
[19] Davey, R.J., Black, S.N., Bromley, L.A., Cottier, D., Dobbs, D.B. and Rout, J.E. (1991) "Molecular design based on recognition at inorganic surfaces", *Nature* **353**, 549.
[20] Falini, G.A., Albeck, S., Weiner, S. and Addadi, L. (1996) "Control of aragonite or calcite polymorphism by mollusc shell macromolecules", *Science* **271**, 67.
[21] Gill, J.S. and Varsanik, R.G. (1986) "Computer modeling of the specific matching between scale inhibitors and crystal-structure of scale forming minerals", *J. of Crystal Growth*, 76.
[22] Parker, S.C., de Leeuw, N.H. and Redfern, S.E. (1999) "Atomistic simulation of oxide surfaces and their reactivity with water", *Faraday Discuss.* **114**, 381.
[23] de Leeuw, N.H., Parker, S.C. and Harding, J.H. (1999) "Molecular dynamics simulation of crystal dissolution from calcite steps", *Phys. Rev. B* **60**, 13792.
[24] Parker, S.C., Oliver, P.M., De Leeuw, N.H., Titiloye, J.O. and Watson, G.W. (1997) "Atomistic simulation of mineral surfaces: Studies of surface stability and growth", *Phase Transitions* **61**, 83.
[25] Oliver, P.M., Watson, G.W. and Parker, S.C. (1995) "Molecular-dynamics simulations of nickel–oxide surfaces", *Physical Review B—Condensed Matter* **52**, 5323.
[26] Parker, S.C., Titoloye, J.O. and Watson, G.W. (1993) "Molecular modeling of carbonate minerals—studies of growth and morphology", *Phil. Trans. Royal Soc. Lon. Ser. A* **344**, 1670.
[27] Gasteiger, J. and Marsili, M. (1980) "Iterative partial equalization of orbital electronegativity—a rapid access to atomic charges", *Tetrahedron* **36**, 3219.
[28] Cerius^2 version 4.0; Molecular Simulations (1998).
[29] Ojo, S. (2002). PhD Thesis, University of London.
[30] Gay, D.H. and Rohl, A.L. (1995) "MARVIN—a new computer code for studying surfaces and interfaces and its application to calculating the crystal morphologies of corundum and zircon", *J. Chem. Soc., Faraday Trans.* **91**, 925.

[31] Pavese, A., Catti, M., Price, G.D. and Jackson, R.A. (1992) "Interatomic potentials for CaCO3 polymorphs (calcite and aragonite), fitted to elastic and vibrational data", *Phys. and Chem. of Min.* **19**, 80.
[32] Dove, P.M. and Hochella, Jr, M.F. (1993) "Calcite precipitation mechanisms and inhibition by orthophosphate—*in situ* observations by scanning force microscopy", *Geochimica et Cosmocim. Acta* **57**, 705.
[33] Mann, S., Didymus, J.M., Sanderson, N.P., Heywood, B.R. and Samper, E.J.A. (1990) "Morphological influence of functionalized and non-functionalized-alpha,omega-dicarboxylates on calcite crystallization", *J. Chem. Soc. Faraday Trans.* **86**, 1873.